Journal of the American College of Cardiology Vol. 56, No. 2, 2010

Published by Elsevier Inc.
ISSN 0735-1097/$36.00
doi:10.1016/j.jacc.2010.02.047

STATE-OF-THE-ART PAPER

Assessment of Nonischemic Myocardial Fibrosis

Christine Jellis, MD,* Jennifer Martin, MD, PhD,* Jagat Narula, MD, PhD,†
Thomas H. Marwick, MD, PhD*‡

Brisbane, Australia; Orange, California; and Cleveland, Ohio

Myocardial fibrosis is recognized as the pathologic entity of extracellular matrix remodeling. Diffuse, reactive fibrosis is being increasingly recognized in a variety of conditions despite the absence of ischemia. Regardless of the etiology, fibrosis leads to increased myocardial stiffness thereby promoting cardiac dysfunction. This may present clinically with symptoms of cardiac failure although often this is a subclinical disease. Various imaging modalities and collagen biomarkers have been used as surrogate markers to assess the presence, extent, and turnover of myocardial fibrosis. Techniques using echocardiography, cardiac magnetic resonance, and nuclear imaging have been developed to detect early features of systolic and diastolic left ventricular dysfunction and impaired contractile reserve. Further identification of diffuse reactive fibrosis may be possible with evolving cardiac magnetic resonance and molecular techniques. The goal of these approaches is to enable targeted therapy to be instituted earlier, leading to prevention of disease progression and fibrosis accumulation long term.
(J Am Coll Cardiol 2010;56:89–97) © 2010 by the American College of Cardiology Foundation

Myocardial fibrosis is a pathological entity of extracellular matrix (ECM) remodeling, often leading to increased myocardial stiffness (1), which may promote abnormalities of cardiac function (2,3). Fibrosis is most commonly found in the setting of ischemic scar, but there is increasing recognition of diffuse myocardial fibrosis occurring as a separate entity in a variety of conditions in the absence of ischemia, including hypertensive heart disease and diabetic, hypertrophic cardiomyopathy (HCM) and idiopathic dilated cardiomyopathy (DCM).

Pathological Fibrosis

ECM is synthesized and degraded in a process of continual tissue growth and repair. This structural scaffolding is constituted in part from fibrillar collagen, which provides both strength and elasticity. Pro-collagen molecules are long, stiff, helical structures composed of 3 alpha chains each containing approximately 1,000 amino acid residues (4). This ropelike structure is typical for collagens found in connective tissue and the myocardium. Types I and III collagen predominate in the heart and have exaggerated accumulation in the settings of hypertension and diabetes (where type III synthesis is proportionally increased by hyperglycemia) (5,6).

Pro-collagen molecules are synthesized within the endoplasmic reticulum of fibroblasts before being secreted into the interstitial space where they undergo cleavage of their end-terminal pro-peptide sequences by pro-collagen N- and C-proteinases (PCP) to enable collagen fiber formation (7) (Fig. 1). The activity of the fibrotic process may be characterized because quantification of cleaved pro-peptide correlates with the amount of fibrillar collagen deposited. Activity of PCP is significantly accelerated by PCP enhancer proteins (PCPE-1, PCPE-2), which are found in connective tissue and the myocardium. Up-regulation of myocardial PCPE-1 has been demonstrated by transforming growth factor beta and aldosterone in rat models with down-regulation of PCPE-1 and collagen deposition noted after spironolactone therapy (8). Several processes in collagen synthesis including inhibition of PCPE or pro-peptide cleavage may provide novel targets for specific cardiac antifibrotic therapy.

After cleavage of pro-peptides, resultant collagen molecules are relatively less soluble and initiate self-assembly into collagen fibrils that then aggregate to form collagen fibers. Fibrils are strengthened by cross-links formed between lysine and hydroxylysine residues within and between collagen molecules. This is facilitated by deamination of residues by lysyl oxidase, yielding aldehyde groups that react to form covalent bonds (9). Advanced glycation end products (AGE), which accumulate with aging and diabetes, have been demonstrated to form AGE-mediated cross-links in collagen resulting in increased arterial stiffness and resistance to enzymatic degradation (9). *N*-epsilon-carboxymethyl-lysine is a major AGE that, with the use of a monoclonal anti-*N*-epsilon-carboxymethyl-lysine antibody, has been demonstrated to be significantly higher in the small intramyocardial arteries of diabetic patients independent of age (10). This microangi-

From the *University of Queensland, Brisbane, Australia; †University of California-Irvine, Orange, California; and the ‡Cleveland Clinic, Cleveland, Ohio.

Manuscript received November 13, 2009; revised manuscript received January 19, 2010, accepted February 1, 2010.

Abbreviations and Acronyms

AGE = advanced glycation end-products

CMR = cardiac magnetic resonance imaging

CRIP = Cy5.5-RGD imaging peptide

ECM = extracellular matrix

HCM = hypertrophic cardiomyopathy

LV = left ventricular

MI = myocardial infarction

MMP = matrix metalloproteinases

PCP = pro-collagen N- and C-proteinases

PCPE = pro-collagen proteinase enhancer protein

PICP = carboxy-terminal pro-peptide of pro-collagen type I

TIMP = tissue inhibitors of metalloproteinases

opathy may also contribute to underlying fibrosis found in diabetic cardiomyopathy.

Collagen turnover is regulated by proteolytic enzymes (matrix metalloproteinases [MMP] and tissue inhibitors of metalloproteinases [TIMP]) and matricellular proteins such as secreted protein, acidic and rich in cysteine (SPARC). The major MMPs expressed in the vasculature include MMP-1, -2, and -9, with MMP-1 having the highest affinity for fibrillar collagen (11). There are 4 known TIMPs, with TIMP-1 being the most predominantly expressed in the myocardium of heart failure patients (12). Concentrations of TIMP-1 are also increased in diabetes and hypertension, with associated impaired myocardial contractility on tissue velocity parameters, perhaps supporting its role in pathological fibrosis (13) (Fig. 2). The ratio of circulating MMP/TIMP maintains the equilibrium of collagen deposition and degradation within the myocardium (14). Matricellular proteins modulate cell–ECM interactions, with key roles including collagen fibril assembly and post-synthetic pro-collagen processing (15). Increased SPARC expression has been noted in myocardial fibrosis associated with left ventricular (LV) hypertrophy and myocardial infarction (MI) (15), although the exact relationship requires further determination.

Fibrosis can be reparative or reactive. In transmural myocardial infarction, the protective strength provided by discrete macroscopic fibrotic scar prevents myocardial rupture. In contrast, myocardium remote from ischemic scar is subject to myocyte hypertrophy and diffuse reactive fibrosis in a detrimental process of remodeling (16), which appears not directly related to ischemia-induced necrosis, but which leads to increased ventricular stiffness and reduced contractile reserve. Both types I and III collagen increase at and remote to the infarct, with synthesis by myofibroblasts in the infarcted myocardium and fibroblasts in the noninfarcted territory and temporal precedence of type III turnover (17). Overall, remote fibrosis is a more significant determinant of adverse structural remodeling found in ischemic cardiomyopathy than the infarct scar itself (18).

Reactive fibrosis also occurs in the nonischemic setting. This diffuse fibrosis is a labile process governed by extrinsic factors such as blood glucose, blood pressure, and accumulation of AGE. Diabetic cardiomyopathy, characterized by diffuse myocardial fibrosis and myofibrillar hypertrophy without evidence of valvular, congenital, hypertensive, or ischemic heart disease (19), exemplifies this process. The remainder of this review will address methods for detection and assessment of diffuse, reactive, nonischemic fibrosis.

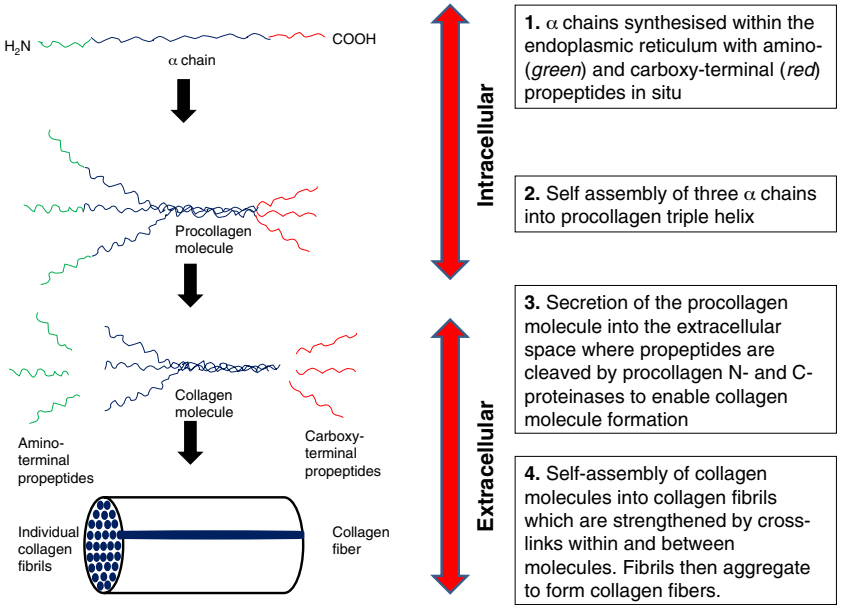

Figure 1 Schematic of Collagen Formation

The diagrams illustrate intracellular and extracellular processes involved in pro-collagen triple-helix synthesis, cleavage of amino- and carboxy-terminal propeptides, and fibrillar collagen fiber formation.

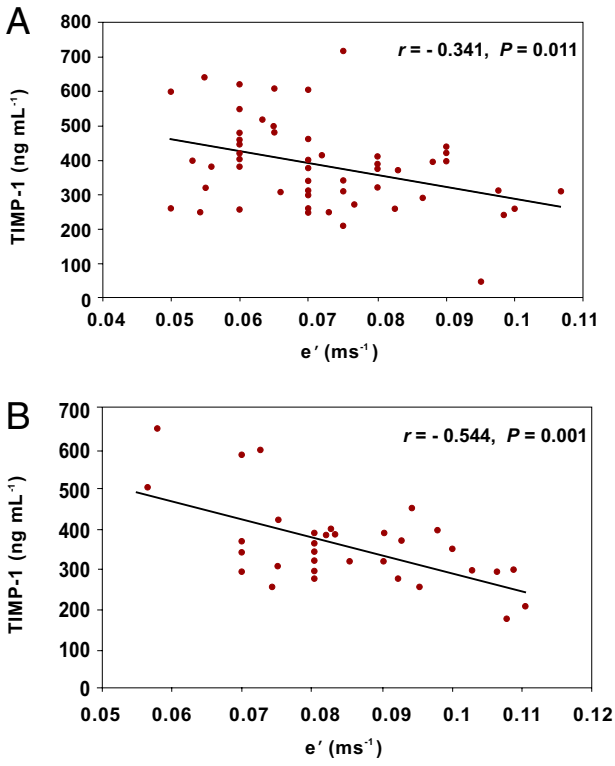

Figure 2 **Relationship Between Myocardial Contractility and Proteolytic Enzymes**

Inverse correlation between tissue inhibitors of metalloproteinases (TIMP)-1 and early diastolic tissue velocity (e′) in patients with **(A)** diabetes and **(B)** hypertension. Reproduced, with permission, from Tayebjee et al. (13).

Noninvasive Assessment of Fibrosis

Although endomyocardial biopsy is the traditional method for quantification of myocardial interstitial collagen content, imaging techniques and serum collagen biomarkers may be used as surrogate markers of myocardial fibrosis (20). These imaging measures may be divided into methods to visualize fibrosis (cardiac magnetic resonance imaging [CMR], nuclear imaging, and integrated backscatter) and techniques to assess subtle subclinical LV systolic and diastolic dysfunction (predominantly echocardiographic). These tools may identify people at risk of cardiac dysfunction from fibrosis, enabling early deployment of antifibrotic therapy.

Many imaging techniques and modalities have been used to assess the presence, extent, and turnover of myocardial fibrosis. Three steps are important. First, to diagnose reactive fibrosis, reparative fibrotic scar and inducible ischemia secondary to coronary artery disease must be excluded. Second, some indirect evidence of fibrosis should be sought—although the noninvasive nature of these tests indicates some degree of inference as they have been validated against myocardial biopsy studies. Third, the assessment may be strengthened by functional evaluation; myocardial fibrosis results in a spectrum of cardiac dysfunction, relating to loss of contractile reserve and abnormal myocardial stiffness, which is proportional to the degree of ECM deposition (Table 1).

Tissue characterization in nonischemic fibrosis. The reflectivity of tissue to ultrasound is a noninvasive measure of myocardial tissue characterization and collagen deposition that has been used for several decades (21). In addition to the qualitative M-mode and 2-dimensional characteristics of scar, such as akinesis and increased acoustic brightness, backscatter techniques were developed in the 1980s to quantify myocardial tissue changes characteristic of fibrosis in conditions such as HCM and hypertension (22). This quantitative echocardiographic estimation of fibrosis was predominantly via ultrasonic videodensitometric and texture analysis. The correlation between backscatter and histologically quantitated collagen has been well validated (23). Noninvasively, amplitudes of integrated backscatter have also been correlated with elevated pro-collagen concentration (24).

Table 1 **Techniques for Noninvasive Assessment of Nonischemic Fibrosis**

Technique	Availability	Ease	Specificity	Quantitative or Functional
Echocardiography				
Backscatter	+++	+++	+++	Quantitative
Tissue Doppler imaging	+++	++	+	Functional
Nuclear imaging				
SPECT–molecular labeling	+	+	+++	Quantitative
PET–perfusable tissue index	++	++	+++	Quantitative
Cardiac magnetic resonance				
Delayed enhancement	+++	++	+++	Quantitative
T_1 mapping	+	++	+++	Quantitative
Tissue tagging	++	++	+	Functional
Collagen biomarkers				
PICP	+	++	++	Quantitative
MMP-1/TIMP-1	+	++	++	Quantitative

+++ = high; ++ = medium; + = low; MMP-1/TIMP-1 = ratio of matrix metalloproteinase type 1 to tissue inhibitor of metalloproteinase type 1; PET = positron emission tomography; PICP = carboxy-terminal pro-peptide of pro-collagen type I; SPECT = single-photon emission computed tomography.

JACC Vol. 56, No. 2, 2010
July 6, 2010:89–97

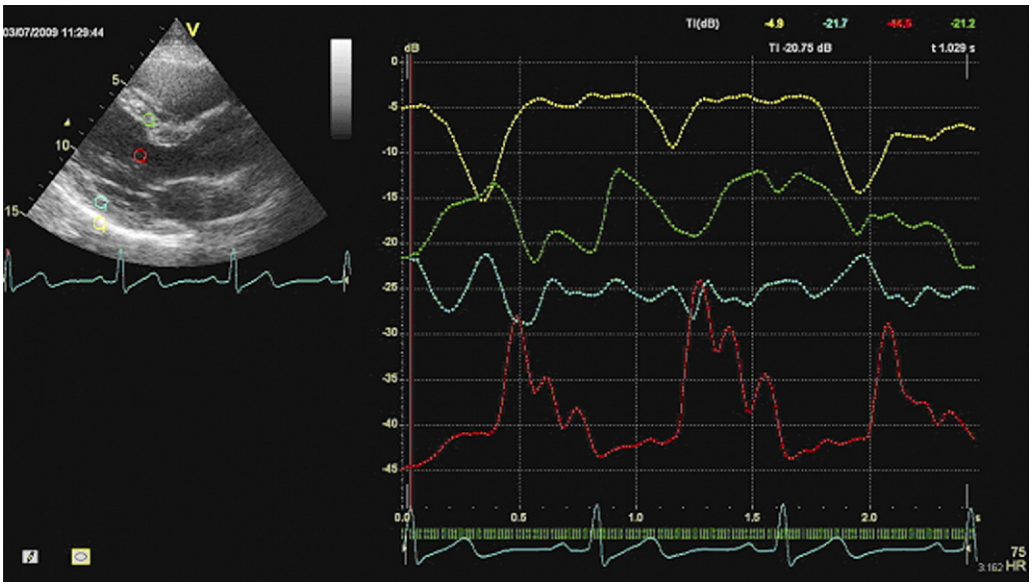

Figure 3 **Calculation of Calibrated Integrated Backscatter**

Measurements of tissue intensity are obtained from sample volumes placed within the pericardium **(yellow)**, posterior wall **(blue)**, and anteroseptum **(green)** in a parasternal long-axis view. A resultant integrated backscatter curve is derived with standard commercial software (Echopac, General Electric Medical Systems, Milwaukee, Wisconsin) and enables calibrated integrated backscatter to be calculated by subtracting mean pericardial integrated backscatter intensity from mean integrated backscatter intensity of the posterior wall or anteroseptum at end diastole.

Two myocardial backscatter parameters have been developed: 1) magnitude of cyclic variation in integrated backscatter; and 2) calibrated integrated backscatter. The former is a marker of regional function, influenced by anisotropy. Although it is abnormal in conditions of diffuse fibrosis (25), it has been superseded by the assessment of myocardial strain. Calibrated integrated backscatter is calculated from tissue intensity curves derived offline (Fig. 3); a greater calibrated integrated backscatter is indicative of greater fibrosis. This technique has been used to establish a transmural trend of fibrosis in partial thickness infarction and hence could potentially be employed to assess fibrotic gradients in conditions, such as diabetic heart disease or Duchenne muscular dystrophy, that have predominantly endocardial or epicardial fibrosis, respectively (26,27). Elevated calibrated integrated backscatter also occurs with systemic sclerosis, although predominantly in the diffuse rather than the limited subgroup (28).

Perfusable tissue index is an indirect marker of fibrosis in both ischemic and nonischemic cardiomyopathies. This measurement is obtainable from the difference between perfusable and nonperfusable tissue on myocardial blood flow imaging with positron emission tomography (29). In idiopathic dilated cardiomyopathy, regional perfusable tissue index correlates with reduced circumferential shortening on magnetic resonance tissue tagging, indicating that myocardial fibrosis is related to impairment in contractile function (30).

ECM turnover. The measurement of pro-collagen-derived pro-peptides to detect myocardial fibrosis turnover offers the attractiveness of simplicity and a short turnaround time (20). However, concentrations can be affected by comorbidities including hepatic impairment, metabolic bone disease, hyperthyroidism, and diabetic nephropathy (31,32). To date, the carboxy-terminal pro-peptide of pro-collagen type I (PICP), amino-terminal pro-peptide of pro-collagen type I, and amino-terminal pro-peptide of pro-collagen type III have been used as markers of collagen turnover in conditions including: diastolic dysfunction, diabetes, hypertension, and idiopathic dilated cardiomyopathy (20,32–34). There is a graded association between PICP in peripheral blood and coronary sinus blood, which is correlated with myocardial collagen content (35), supporting its use as a biomarker of collagen type-1 turnover. This association has not been validated for other pro-peptides. A strong association between collagen volume fraction on endomyocardial biopsy and serum PICP has previously been identified in hypertension (31). When used with an echocardiogram, fibrosis detection may be further improved as demonstrated by the association between backscatter and increased PICP (24). Like PICP, the measurable gradient of TIMP-1 and MMP-1 from coronary sinus to peripheral blood supports their use as biomarkers (36).

Interstitial alterations including myofibroblastic proliferation have been demonstrated remote to scar in post-MI ventricular remodeling (16). Overexpression of myofibro-

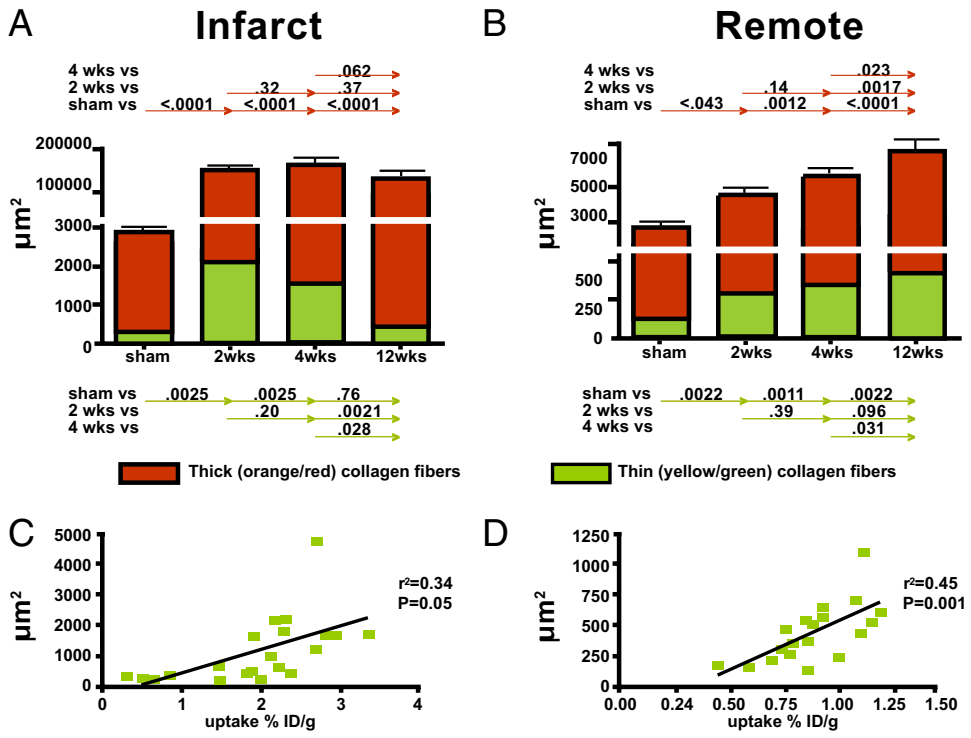

Figure 4 **Collagen Types in the Infarct and Remote Regions**

Temporal characterization of collagen fibers by polarization revealed that the thin or new collagen fibers **(green)** decreased in the infarct region (suggesting collagen maturation) **(A)** and increased in the remote area **(B)** (suggesting ongoing new collagen production). The prevalence of new collagen fibers paralleled the Cy5.5-RGD imaging peptide uptake in both infarct and remote zones **(C, D)**. Adapted, with permission, from van den Borne et al. (39).

blastic cell membrane moieties in this setting, such as angiotensin receptors and integrins (37), can be exploited with specific fluorescent and/or radiotracer labeling to localize myofibroblasts on fluorescence or micro-single-photon emission computed tomography imaging. Such targeted imaging has been performed in the murine post-MI model using a fluoresceinated angiotensin peptide analog and radiolabeled angiotensin II receptor blocker (technetium-99m losartan) to demonstrate distinct uptake in the infarct area up to 12 weeks after the event (38). This targeted myofibroblast receptor imaging was verified on pathologic characterization with localization of tracer to collagen-producing myofibroblasts.

Molecular imaging with the RGD peptide (containing the arginine-glycine-aspartate motif), which binds to integrins such as alpha$_v$beta$_3$, has also been used to evaluate myocardial remodeling in post-MI murine models. Specifically, Cy5.5-RGD imaging peptide (CRIP) labeled with technetium-99m has been developed as a surrogate marker of thin, newly formed collagen deposition (39). Importantly, although maximum CRIP uptake was observed in the infarct area, this had halved by 12 weeks, with the uptake then being higher in the peri-infarct zone and remote myocardium, indicative of newly formed collagen fibers reflective of myocardial remodeling (Fig. 4).

CRIP imaging has also been employed to demonstrate the beneficial effect of neurohormonal antagonism on myocardial remodeling post-MI. Captopril, losartan, and spironolactone individually or in combination significantly reduce CRIP uptake in both infarct and remote myocardial zones correlating with improved LV function on echocardiography (40). On histological verification, the extent of interstitial fibrosis in the remote myocardium was significantly decreased whereas collagen maturation in the infarct zone was accelerated, suggesting that neurohormonal antagonists can cause prevention of both remote ventricular remodeling and localized aneurysmal dilation. These molecular imaging techniques could have clinical applications in noninvasive estimation of myocardial fibrosis. The measurement of relative uptake with single-photon emission computed tomography makes them more likely to find application in the assessment of LV remodeling and prediction of heart failure following MI.

Quantification of ECM. CMR imaging has been widely used to detect and assess myocardial scar and perfusion and is the noninvasive gold standard for quantification of focal myocardial fibrosis. Delayed enhancement CMR highlights regions of scar or fibrosis, as small as 0.16 g (41), as an area of high intensity signal (42). Conventionally, this method is performed using inversion recovery gradient-echo sequences

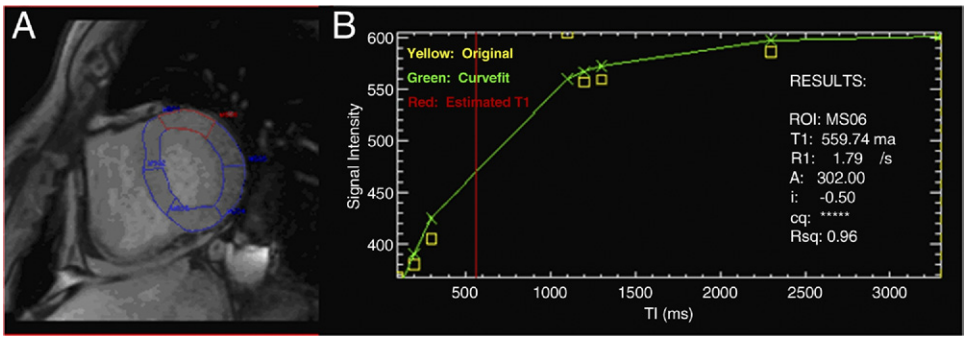

Figure 5 T_1 Mapping for Fibrosis

This post-contrast T_1 map of the basal ventricle in short-axis view is demonstrated with a region of interest delineating the basal anterior segment (MS06) **(A)**. An exponential recovery curve of signal intensities at different inversion times is then produced to determine a post-contrast myocardial T_1 time of 559.74 ms **(red line)** for the basal anterior segment **(B)**.

10 to 15 min after gadolinium infusion. Retention of contrast within the extracellular space results in shortening of the inversion time (T_1) and hyperenhancement relative to normal myocardium. Ischemic scar usually results in delayed enhancement in a subendocardial or transmural distribution consistent with the perfusion territories of epicardial coronary arteries, whereas nonischemic fibrosis tends to be irregular and intramural, even subepicardial, in distribution (43). Fibrosis is frequently identified in LV hypertrophy, and delayed enhancement is associated with the degree of LV remodeling (44) and LV end-diastolic pressure, all of which further supports the role of interstitial fibrosis in impaired relaxation (45).

The main limiting factor with using delayed enhancement CMR in nonischemic cardiomyopathies is that the fibrotic process is often diffuse, thereby lacking the normal nonfibrotic myocardium as a frame of reference. Several new CMR techniques have been used in trials for detection of nonischemic myocardial fibrosis. Development of a multislice, single-shot 2-dimensional phase-sensitive inversion recovery sequence enables faster detection (24 ± 3 s vs. 385 ± 127 s) and quantification of delayed enhancement compared with traditional sequences (46). The use of this T_1-insensitive sequence overcomes the reliance on contrast between abnormal and normal myocardium. Contrast-enhanced T_1 mapping has also been developed to quantify diffuse, nonischemic myocardial fibrosis. Using a modified Look-Locker inversion-recovery prototype sequence (47), a series of short-axis images, typically basal, mid-ventricular, and apical slices divided into segments, are acquired with different inversion times. An exponential recovery curve of signal intensities at different inversion times is then created for each designated segment to determine the post-contrast myocardial T_1 time (Fig. 5). The T_1 time is then employed as an index of diffuse fibrosis with a shorter T_1 time corresponding to increased myocardial fibrosis as previously validated by myocardial biopsy (48) (Fig. 6). By removing reliance on contrasting signal intensity, this method enables detection of diffuse fibrosis.

T_2 relaxation time is another CMR technique employed to assess tissue properties. In diabetic rats, T_2 relaxation time was significantly reduced compared with controls and inversely correlated with collagen fractional area on histology (49). T_2-weighted sequences have also been employed in the diagnosis of isolated LV noncompaction, where apical regions of high intensity are reflective of fibrosis (50). The most sensitive and specific noninvasive method for quantitation of nonischemic reactive fibrosis needs to be established by comparison of the preceding modalities, in particular perfusable tissue index, T_1 mapping, and PICP, against myocardial biopsy.

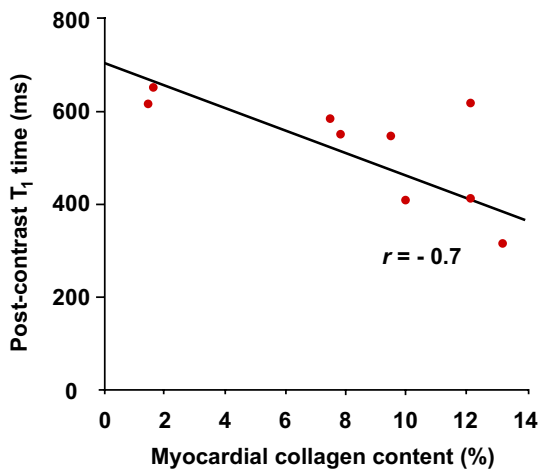

Figure 6 Relationship Between Myocardial Collagen Content and Post-Contrast T_1 Time

Relationship between myocardial collagen content on myocardial biopsy and post-contrast T_1 time on cardiac magnetic resonance imaging. Reproduced, with permission, from Iles et al. (48).

Functional Systolic and Diastolic Assessment

LV ejection fraction, chamber wall thicknesses, and atrial areas give gross estimates of LV function and filling pressures. Tissue Doppler imaging can be used to assess myocardial tissue velocity and deformation parameters as measures of myocardial function that may be reduced in the fibrotic heart. Reduction of longitudinal function appears to be the most sensitive marker of subclinical heart disease in many conditions associated with fibrosis, including diabetes and hypertension. This impairment of longitudinal function reflects the predominant initial involvement of subendocardial fibers, with compensation by mid-wall fibers and resultant improvement in radial contractility to maintain overall cardiac function (26).

Peak systolic and early diastolic myocardial tissue velocities have been used to identify early subclinical disease despite normal conventional echocardiographic values in several progressive, nonischemic fibrotic processes. A reduction in both parameters has been detected in patients with diabetes but no evidence of heart failure, and early diastolic tissue velocity has also been found to be reduced with advancing age and hypertension; angiotensin-converting enzyme inhibitor therapy appears to be protective (51,52). This impairment in myocardial velocity and resultant impaired ventricular relaxation may reflect interstitial fibrosis, altered cardiomyocyte cytoskeleton properties, or a combination of both. This relationship is supported by endomyocardial biopsy findings that inversely relate percent fibrosis to tissue Doppler-derived systolic and early diastolic tissue velocity (53).

It has recently become possible to assess LV mechanics with echocardiographic deformation techniques (strain and strain rate) and magnetic resonance imaging tissue tagging. Strain is a fundamental property of matter that relates to the deformation that occurs after the application of stress (54). It correlates inversely with the degree of LV dysfunction and may become abnormal earlier in cardiomyopathic processes than other echocardiography techniques. Strain and strain rate can be measured using tissue Doppler imaging or 2-dimensional speckle tracking echocardiography. Both methods can detect subclinical heart disease in fibrotic processes, with the predominant planes of strain initially affected mirroring the histological location of early fibrosis. Peak systolic longitudinal strain is typically reduced in diabetes (consistent with initial impairment of endocardial contractility), whereas peak systolic radial strain is impaired in Duchenne muscular dystrophy (an epicardial fibrotic process) (26,55). Impaired deformation parameters have also been noted in conditions including: uncontrolled hypertension with elevated serum TIMP-1 levels and systemic sclerosis with cardiac involvement (28,56). Notably, measures appear to improve in diastolic heart failure after aldosterone antagonism, perhaps reflective of an antifibrotic effect (57). An inverse relationship between deformation parameters and backscatter in LV hypertrophy and diabetes

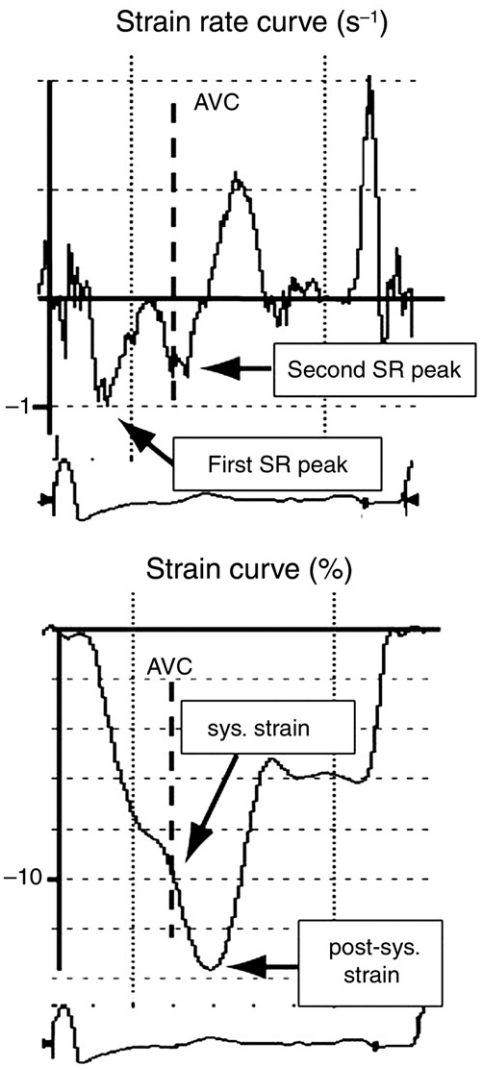

Figure 7 SR Imaging Displaying the "Double Peak Sign"

Longitudinal strain rate curve from a segment with delayed enhancement on cardiac magnetic resonance imaging displaying the "double peak sign" indicative of fibrosis. Reproduced, with permission, from Weidemann et al. (58). AVC = aortic valve closure; CMR = cardiac magnetic resonance imaging; SR = strain rate.

further supports underlying fibrosis as a common pathology (52). In conditions such as severe aortic valve stenosis, Fabry disease, and HCM, regions of delayed enhancement on CMR also display a characteristic systolic pattern on strain-rate imaging termed the "double peak sign" (58) (Fig. 7).

Tagging of myocardial tissue with a matrix of radiofrequency saturation enables tissue tracking and calculation of rotation and displacement in 3 dimensions (59). This CMR technique has been used to assess cardiac motion and deformation in conditions such as HCM, where reduced regional myocardial shortening with increased LV torsion is noted (60). The combination of tissue tagging with delayed enhancement CMR may enable stratification of occult

cardiac dysfunction secondary to fibrosis in muscular dystrophies (61).

Conclusions

Nonischemic fibrosis is being increasingly recognized in multiple etiologies as a pathological entity. Often this manifests as diastolic dysfunction or heart failure with preserved ejection fraction, both of which have important prognostic implications. The ability to simply, rapidly, and accurately identify and quantify the contribution of fibrosis to these disease processes with imaging techniques and biomarkers may allow a more specific and timely strategy to be applied in the treatment of these conditions.

Reprint requests and correspondence: Dr. Thomas H. Marwick, Cardiovascular Imaging J1-5, Heart and Vascular Institute, Cleveland Clinic, 9500 Euclid Avenue, Cleveland, Ohio 44195. E-mail: marwict@ccf.org.

REFERENCES

1. Sugihara N, Genda A, Shimizu M, et al. [Diastolic dysfunction and its relation to myocardial fibrosis in essential hypertension]. J Cardiol 1988;18:353–61.
2. Diez J. Mechanisms of cardiac fibrosis in hypertension. J Clin Hypertens (Greenwich) 2007;9:546–50.
3. McLenachan JM, Dargie HJ. Ventricular arrhythmias in hypertensive left ventricular hypertrophy. Relationship to coronary artery disease, left ventricular dysfunction, and myocardial fibrosis. Am J Hypertens 1990;3:735–40.
4. van der Rest M, Garrone R. Collagen family of proteins. FASEB J 1991;5:2814–23.
5. Pardo Mindan FJ, Panizo A. Alterations in the extracellular matrix of the myocardium in essential hypertension. Eur Heart J 1993;14 Suppl J:12–4.
6. Shimizu M, Umeda K, Sugihara N, et al. Collagen remodelling in myocardia of patients with diabetes. J Clin Pathol 1993;46:32–6.
7. Weber KT. Monitoring tissue repair and fibrosis from a distance. Circulation 1997;96:2488–92.
8. Kessler-Icekson G, Schlesinger H, Freimann S, Kessler E. Expression of procollagen C-proteinase enhancer-1 in the remodeling rat heart is stimulated by aldosterone. Int J Biochem Cell Biol 2006;38:358–65.
9. Robins SP. Biochemistry and functional significance of collagen cross-linking. Biochem Soc Trans 2007;35:849–52.
10. Schalkwijk CG, Baidoshvili A, Stehouwer CD, van Hinsbergh VW, Niessen HW. Increased accumulation of the glycoxidation product Nepsilon-(carboxymethyl)lysine in hearts of diabetic patients: generation and characterisation of a monoclonal anti-CML antibody. Biochim Biophys Acta 2004;1636:82–9.
11. Visse R, Nagase H. Matrix metalloproteinases and tissue inhibitors of metalloproteinases: structure, function, and biochemistry. Circ Res 2003;92:827–39.
12. Barton PJ, Birks EJ, Felkin LE, Cullen ME, Koban MU, Yacoub MH. Increased expression of extracellular matrix regulators TIMP1 and MMP1 in deteriorating heart failure. J Heart Lung Transplant 2003;22:738–44.
13. Tayebjee MH, Lim HS, Nadar S, MacFadyen RJ, Lip GY. Tissue inhibitor of metalloproteinse-1 is a marker of diastolic dysfunction using tissue Doppler in patients with type 2 diabetes and hypertension. Eur J Clin Invest 2005;35:8–12.
14. Cleutjens JP. The role of matrix metalloproteinases in heart disease. Cardiovasc Res 1996;32:816–21.
15. McCurdy S, Baicu CF, Heymans S, Bradshaw AD. Cardiac extracellular matrix remodeling: fibrillar collagens and Secreted Protein Acidic and Rich in Cysteine (SPARC). J Mol Cell Cardiol 2010;48:544–9.
16. Swynghedauw B. Molecular mechanisms of myocardial remodeling. Physiol Rev 1999;79:215–62.
17. Cleutjens JP, Verluyten MJ, Smiths JF, Daemen MJ. Collagen remodeling after myocardial infarction in the rat heart. Am J Pathol 1995;147:325–38.
18. Beltrami CA, Finato N, Rocco M, et al. Structural basis of end-stage failure in ischemic cardiomyopathy in humans. Circulation 1994;89:151–63.
19. Rubler S, Dlugash J, Yuceoglu YZ, Kumral T, Branwood AW, Grishman A. New type of cardiomyopathy associated with diabetic glomerulosclerosis. Am J Cardiol 1972;30:595–602.
20. Martos R, Baugh J, Ledwidge M, et al. Diastolic heart failure: evidence of increased myocardial collagen turnover linked to diastolic dysfunction. Circulation 2007;115:888–95.
21. Mimbs JW, O'Donnell M, Bauwens D, Miller JW, Sobel BE. The dependence of ultrasonic attenuation and backscatter on collagen content in dog and rabbit hearts. Circ Res 1980;47:49–58.
22. Shapiro LM, Moore RB, Logan-Sinclair RB, Gibson DG. Relation of regional echo amplitude to left ventricular function and the electrocardiogram in left ventricular hypertrophy. Br Heart J 1984;52:99–105.
23. Picano E, Pelosi G, Marzilli M, et al. In vivo quantitative ultrasonic evaluation of myocardial fibrosis in humans. Circulation 1990;81:58–64.
24. Lin YH, Shiau YC, Yen RF, et al. The relation between myocardial cyclic variation of integrated backscatter and serum concentrations of procollagen propeptides in hypertensive patients. Ultrasound Med Biol 2004;30:885–91.
25. Ferri C, Di Bello V, Martini A, et al. Heart involvement in systemic sclerosis: an ultrasonic tissue characterisation study. Ann Rheum Dis 1998;57:296–302.
26. Fang ZY, Leano R, Marwick TH. Relationship between longitudinal and radial contractility in subclinical diabetic heart disease. Clin Sci (Lond) 2004;106:53–60.
27. Naito J, Masuyama T, Mano T, et al. Analysis of transmural trend of myocardial integrated ultrasonic backscatter in patients with old myocardial infarction. Ultrasound Med Biol 1996;22:807–14.
28. Mele D, Censi S, La Corte R, et al. Abnormalities of left ventricular function in asymptomatic patients with systemic sclerosis using Doppler measures of myocardial strain. J Am Soc Echocardiogr 2008;21:1257–64.
29. Knaapen P, Boellaard R, Gotte MJ, et al. Perfusable tissue index as a potential marker of fibrosis in patients with idiopathic dilated cardiomyopathy. J Nucl Med 2004;45:1299–304.
30. Knaapen P, Gotte MJ, Paulus WJ, et al. Does myocardial fibrosis hinder contractile function and perfusion in idiopathic dilated cardiomyopathy? PET and MR imaging study. Radiology 2006;240:380–8.
31. Querejeta R, Varo N, Lopez B, et al. Serum carboxy-terminal propeptide of procollagen type I is a marker of myocardial fibrosis in hypertensive heart disease. Circulation 2000;101:1729–35.
32. Inukai T, Fujiwara Y, Tayama K, Aso Y, Takemura Y. Serum levels of carboxy-terminal propeptide of human type I procollagen are an indicator for the progression of diabetic nephropathy in patients with type 2 diabetes mellitus. Diabetes Res Clin Pract 2000;48:23–8.
33. Klappacher G, Franzen P, Haab D, et al. Measuring extracellular matrix turnover in the serum of patients with idiopathic or ischemic dilated cardiomyopathy and impact on diagnosis and prognosis. Am J Cardiol 1995;75:913–8.
34. Brilla CG, Matsubara L, Weber KT. Advanced hypertensive heart disease in spontaneously hypertensive rats. Lisinopril-mediated regression of myocardial fibrosis. Hypertension 1996;28:269–75.
35. Gonzalez A, Lopez B, Ravassa S, et al. Biochemical markers of myocardial remodelling in hypertensive heart disease. Cardiovasc Res 2009;81:509–18.
36. Lopez B, Gonzalez A, Querejeta R, Larman M, Diez J. Alterations in the pattern of collagen deposition may contribute to the deterioration of systolic function in hypertensive patients with heart failure. J Am Coll Cardiol 2006;48:89–96.
37. Asano Y, Ihn H, Yamane K, Jinnin M, Mimura Y, Tamaki K. Increased expression of integrin alpha(v)beta3 contributes to the establishment of autocrine TGF-beta signaling in scleroderma fibroblasts. J Immunol 2005;175:7708–18.
38. Verjans JW, Lovhaug D, Narula N, et al. Noninvasive imaging of angiotensin receptors after myocardial infarction. J Am Coll Cardiol Img 2008;1:354–62.

39. van den Borne SW, Isobe S, Verjans JW, et al. Molecular imaging of interstitial alterations in remodeling myocardium after myocardial infarction. J Am Coll Cardiol 2008;52:2017–28.
40. van den Borne SW, Isobe S, Zandbergen HR, et al. Molecular imaging for efficacy of pharmacologic intervention in myocardial remodeling. J Am Coll Cardiol Img 2009;2:187–98.
41. Wu E, Judd RM, Vargas JD, Klocke FJ, Bonow RO, Kim RJ. Visualisation of presence, location, and transmural extent of healed Q-wave and non-Q-wave myocardial infarction. Lancet 2001;357: 21–8.
42. Dulce MC, Duerinckx AJ, Hartiala J, et al. MR imaging of the myocardium using nonionic contrast medium: signal-intensity changes in patients with subacute myocardial infarction. AJR Am J Roentgenol 1993;160:963–70.
43. Gottlieb I, Macedo R, Bluemke DA, Lima JA. Magnetic resonance imaging in the evaluation of non-ischemic cardiomyopathies: current applications and future perspectives. Heart Fail Rev 2006;11:313–23.
44. Rudolph A, Abdel-Aty H, Bohl S, et al. Noninvasive detection of fibrosis applying contrast-enhanced cardiac magnetic resonance in different forms of left ventricular hypertrophy relation to remodeling. J Am Coll Cardiol 2009;53:284–91.
45. Andersen K, Hennersdorf M, Cohnen M, Blondin D, Modder U, Poll LW. Myocardial delayed contrast enhancement in patients with arterial hypertension: initial results of cardiac MRI. Eur J Radiol 2009;71:75–81.
46. Elgeti T, Abdel-Aty H, Wagner M, et al. Assessment of late gadolinium enhancement in nonischemic cardiomyopathy: comparison of a fast Phase-Sensitive Inversion Recovery Sequence (PSIR) and a conventional segmented 2D gradient echo recall (GRE) sequence—preliminary findings. Invest Radiol 2007;42:671–5.
47. Messroghli DR, Greiser A, Frohlich M, Dietz R, Schulz-Menger J. Optimization and validation of a fully-integrated pulse sequence for modified look-locker inversion-recovery (MOLLI) T1 mapping of the heart. J Magn Reson Imaging 2007;26:1081–6.
48. Iles L, Pfluger H, Phrommintikul A, et al. Evaluation of diffuse myocardial fibrosis in heart failure with cardiac magnetic resonance contrast-enhanced T1 mapping. J Am Coll Cardiol 2008;52:1574–80.
49. Loganathan R, Bilgen M, Al-Hafez B, Smirnova IV. Characterization of alterations in diabetic myocardial tissue using high resolution MRI. Int J Cardiovasc Imaging 2006;22:81–90.
50. Hamamichi Y, Ichida F, Hashimoto I, et al. Isolated noncompaction of the ventricular myocardium: ultrafast computed tomography and magnetic resonance imaging. Int J Cardiovasc Imaging 2001;17: 305–14.
51. Fang ZY, Schull-Meade R, Downey M, Prins J, Marwick TH. Determinants of subclinical diabetic heart disease. Diabetologia 2005; 48:394–402.
52. Fang ZY, Yuda S, Anderson V, Short L, Case C, Marwick TH. Echocardiographic detection of early diabetic myocardial disease. J Am Coll Cardiol 2003;41:611–7.
53. Shan K, Bick RJ, Poindexter BJ, et al. Relation of tissue Doppler derived myocardial velocities to myocardial structure and beta-adrenergic receptor density in humans. J Am Coll Cardiol 2000;36: 891–6.
54. Mirsky I, Parmley WW. Assessment of passive elastic stiffness for isolated heart muscle and the intact heart. Circ Res 1973;33:233–43.
55. Mori K, Hayabuchi Y, Inoue M, et al. Myocardial strain imaging for early detection of cardiac involvement in patients with Duchenne's progressive muscular dystrophy. Echocardiography 2007;24: 598–608.
56. Kang SJ, Lim HS, Choi BJ, et al. Longitudinal strain and torsion assessed by two-dimensional speckle tracking correlate with the serum level of tissue inhibitor of matrix metalloproteinase-1, a marker of myocardial fibrosis, in patients with hypertension. J Am Soc Echocardiogr 2008;21:907–11.
57. Mottram PM, Haluska B, Leano R, Cowley D, Stowasser M, Marwick TH. Effect of aldosterone antagonism on myocardial dysfunction in hypertensive patients with diastolic heart failure. Circulation 2004;110:558–65.
58. Weidemann F, Niemann M, Herrmann S, et al. A new echocardiographic approach for the detection of non-ischaemic fibrosis in hypertrophic myocardium. Eur Heart J 2007;28:3020–6.
59. Zerhouni EA, Parish DM, Rogers WJ, Yang A, Shapiro EP. Human heart: tagging with MR imaging—a method for noninvasive assessment of myocardial motion. Radiology 1988;169:59–63.
60. Young AA, Kramer CM, Ferrari VA, Axel L, Reichek N. Three-dimensional left ventricular deformation in hypertrophic cardiomyopathy. Circulation 1994;90:854–67.
61. Hor KN, Wansapura J, Markham LW, et al. Circumferential strain analysis identifies strata of cardiomyopathy in Duchenne muscular dystrophy: a cardiac magnetic resonance tagging study. J Am Coll Cardiol 2009;53:1204–10.

Key Words: fibrosis ■ myocardial ■ heart failure.